Probabilistic seismic performance and loss assessment of a bridge-foundation-soil system

B.A. Bradley.
GNS Science, Lower Hutt, New Zealand

M. Cubrinovski, R.P. Dhakal, G.A. MacRae
Department of Civil and Natural Resources Engineering, University of Canterbury, New Zealand

ABSTRACT: This paper presents the probabilistic seismic performance assessment of an actual bridge-foundation-soil system, the Fitzgerald Avenue twin bridges. A two-dimensional plane strain finite element model of the longitudinal direction of the bridge-foundation-soil system is modeled using advanced soil and structural constitutive models. Ground motions are selected based on the seismic hazard deaggregation at the site, which is dominated by both fault and distributed seismicity. Based on rigorous examination of several deterministic analyses, engineering demand parameters (EDP's) are determined which capture the global and local demand and damage to the bridge and foundation, and multiple ground motions at various intensity levels are used to conduct seismic response analyses of the system. A probabilistic seismic loss assessment of the structure considering both direct repair and loss of functionality consequences was performed to holistically assess the seismic risk of the system. It was found that the non-horizontal layering of the sedimentary soils has a pronounced effect on the seismic demand distribution to the bridge components, of which the north abutment piles and central pier are critical in the systems seismic performance. The consequences due to loss of functionality of the bridge during repair were significantly larger than the direct repair costs, with over a 2% in 50 year probability of the total loss exceeding twice the book-value of the structure.

1 INTRODUCTION

Methods for assessment of the seismic performance of soil-structure systems have evolved significantly in the past two decades. This evolution has involved further improvement of simplified design-oriented approaches, and also development of more robust, and complex, analysis procedures. In addition to the development in methods of analysis, attention has shifted from the implicit assessment of seismic performance via seismic response analysis, to an explicit consideration of seismic performance based on the consequences of seismic response and associated damage.

Consideration of the seismic response of soil-structure systems is complicated by the complexity of the ground motion excitation and the non-linear dynamic response of soil-structure systems. In addition to this complexity, the seismic response of soil-structure systems is burdened by a significant amount of uncertainty. Such uncertainty arises due to the uncertain nature of future ground motions which will occur at the site, as well as the lack of knowledge of the properties governing the response of the soil-structure system. In addition to the ground motion and seismic response uncertainties there are also uncertainties associated with the levels of damage to the structure and the corresponding consequences in terms of direct repair costs and loss of functionality and human injuries.

Recent efforts (Bradley et al. 2009b), predominantly following the Pacific Earthquake Engineering Research (PEER) Centre framework formula have focused on performance-based methodologies which allows the computation of seismic performance measures encompassing direct and indirect consequences associated with the seismic response of engineered facilities as well as addressing the significant aforementioned uncertainties in the seismic assessment problem.

The focus of this paper is the probabilistic seismic performance assessment of a two-span bridge structure supported on pile foundations which are founded in liquefiable soils. Firstly, the structure, site conditions, and computational model of the soil-pile-bridge system are discussed. An overview of the seismic response of the system for a single ground motion is discussed to elucidate the predominant deformation mechanisms of the system and to identify the engineering demand parameters (EDP's) to use in the probabilistic seismic demand assessment. Ground motions are selected in accordance with the seismic hazard deaggregation for various intensity levels, and the results of the seismic response analyses are used to perform probabilistic seismic demand assessments of the system.

2 CASE STUDY: FITZGERALD AVENUE BRIDGES

2.1 *Details of the structure*

The Fitzgerald Avenue twin bridges are located near to the north-west of central Christchurch, New Zealand. Each of the two-span bridges is 30 m long, 12.1 m wide and 3.2 m high (Figure 1a). The 15 m bridge deck spans consist of 21 prestressed concrete I-girders and cast-in-place concrete slabs. The bridge superstructure is supported on two seat abutments and one central pier (Figure 1b). The abutments and pier which are 2.5 m and are the same width as the superstructure deck and are supported on pile group foundation consisting of eight - 0.3 m diameter piles. All piles have continuous moment connections at the pile cap. At both abutments the bridge deck is seated on a 10 mm bearing pad as illustrated in Figure 1c.

Because of their location in the transportation network, the Fitzgerald Avenue bridges have been designated by the Christchurch City Council as a key lifeline for post-earthquake transportation. A recent assessment of the bridge structure recommended the installation of two additional driven piles at each of the abutments and central pier to a depth of 25 m. The two piles on each side of the central pier are 1.5 m in diameter, while those at the abutments are 1.2 m in diameter.

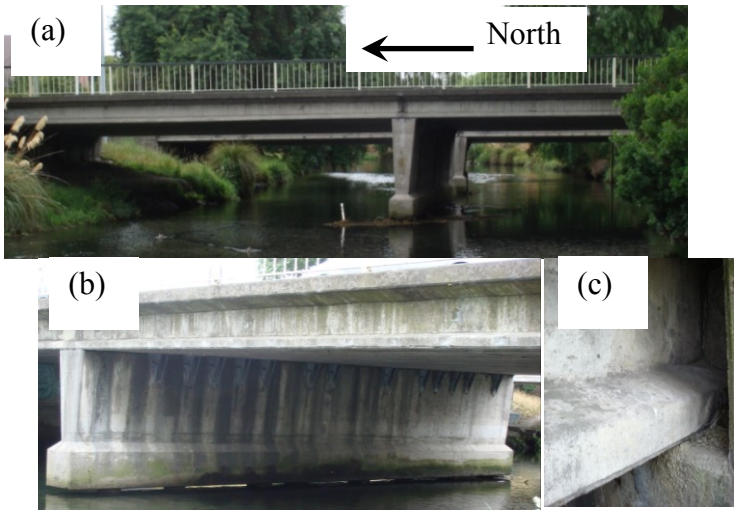

Figure 1: The Fitzgerald Avenue twin bridges: (a) elevation of the west bridge; (b) illustration of the central pier and pile cap; and (c) seating connection of bridge deck on abutments.

2.2 *Site conditions*

Previous site investigations conducted to confirm ground conditions and assess material strengths and liquefaction potential include: boreholes with standard penetrometer tests (SPT's); cone penetrometer tests (CPT's) with direct push Dual Tubes (DT's); and installation of piezometers. Based on these site investigations, the generic soil profile for the longitudinal axis of the bridge given in Figure 2 was developed. The soil profile consists of four distinct layers. The shallowest two horizontal layers have thicknesses of 4.5 m and 6.5 m, and normalised SPT blowcounts of $N_1 = 10$ and $N_1 = 15$, respectively. Below these two layers, the profile deviates from a simple horizontal layering, with a weaker layer of 6.5 m depth and SPT blowcount of $N_1 = 10$ on the left hand side of the model. Below 17.5 m on the left hand side of the model, and up to 11m depth on the right hand side of the model is a significantly stiffer layer of $N_1 = 30$. Both the $N_1 = 10$ and $N_1 = 15$ layers are highly susceptible to liquefaction, while the $N_1 = 30$ base layer was deemed to be of a significantly lower liquefaction potential. Behind the abutments, gravel backfills extend at an angle of 30 degrees above horizontal to the surface.

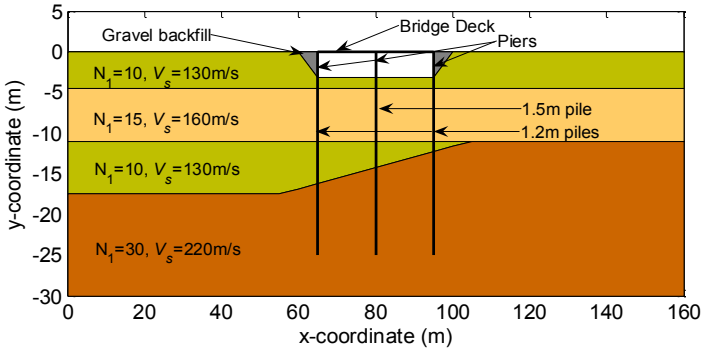

Figure 2: Schematic illustration of generic soil profile used in the computational model.

3 COMPUTATIONAL MODEL

A non-linear finite element plane-strain model of longitudinal direction of the bridge-foundation-soil system was constructed in the finite element program Diana-J (1987). While the seismic response of the bridge-pile-soil system is clearly a 3-dimensional problem, only the analyses of the longitudinal direction are discussed herein. Details of the effective stress analyses of the transverse direction of the bridge system are presented in Bowen and Cubrinovski (2008) and Cubrinovski and Bradley (2009).

Because of symmetry, the out-of-plane width of the longitudinal plane-strain model was taken to be half of the bridge width (6.05 m). That is, half of the bridge deck, abutments and piers were considered, as well as the same dimension for the soil thickness. Therefore, in the computational model, each abutment and pier is supported by a single 1.2 m and 1.5 m pile, respectively. The 0.3 m diameter piles (length 9.5m) which supported the structure before the installation of the 1.2 m and 1.5 m piles provide negligible contribution to the stiffness and strength of the pile group and were not considered in the computational model.

Because of the high liquefaction potential of the foundation soil, its dynamic response was considered to be a dominant feature affecting the response of the bridge-pile-soil system. The soil was modelled using the two-phase (soil-water) Stress-Density (S-D) constitutive model of Cubrinovski and Ishihara (1998). Further details on the computation of the

constitutive model parameters used in the analysis is given in Bowen and Cubrinovski (2008) and Cubrinovski and Ishihara (1998).

The bridge abutments, central pier and pile foundations were modelled using displacement-based beam elements with three gauss points. At each gauss point, the moment-curvature response was parameterized by a hyperbolic curve, with the initial stiffness, EI, and peak moment, M_F, chosen to match the moment curvature relationship of the pile (See Bowen and Cubrinovski (2008) for details). The unloading/reloading path for the moment-curvature relationship is based on the Masing rule, and no strength degradation was considered due to limitations of the constitutive model. The bridge superstructure was modelled as linear elastic because of its significantly higher axial stiffness compared to the lateral stiffness of the abutments/piers and its higher flexural and shear strength.

A static analysis was performed in order to determine the initial stress distribution in the model. In particular, a correct distribution of shear stresses near the abutments is critical for modelling the tendency for lateral spreading of soil toward the river channel.

In addition to hysteretic damping occurring as a result of the inelastic constitutive models, Rayleigh damping was used to provide enhanced numerical stability with parameters $\alpha = 0$ and $\beta = 0.005$.

4 SEISMIC HAZARD AND GROUND MOTIONS

The seismic hazard due to earthquake-induced ground motion is determined using probabilistic seismic hazard analysis (PSHA). In order to obtain the seismic hazard curve it is first necessary to specify which ground motion intensity measure (IM) is to be used. In this study, PGA is used as the IM, both for its historical use and because it and spectral accelerations at various periods are the only IM's for which seismic hazard curves are publicly available for this location. Recent studies (Bradley et al. 2009a) have shown however that velocity-based IM's (e.g. peak ground velocity, PGV, and spectrum intensity, SI) are better IM's for such analyses of structures in liquefiable soils.

Figure 3a illustrates the ground motion hazard at the site of the bridge structure, while Figure 3b illustrates the hazard deaggregation used for ground motion selection. Ground motion selection in accordance with the seismic hazard deaggregation has been shown important (Shome & Cornell 1999), particularly for inefficient and insufficient IM's such as PGA. As noted by Stirling et al. (2007) and evident in Figure 3b the seismic hazard is dominated by: (i) $M_W = 5.5$-6.5 earthquakes at short distances ($R = 15$-30 km), associated with background seismicity, and (ii) larger ($M_W = 7$-7.5) earthquakes on mapped faults ranging from $R = 25$-50 km.

Ground motions were selected for seismic response analyses at 9 different intensity levels as shown in Figure 3a. For each intensity level, ground motions were selected from the NGA database (http://peer.berkley.edu/nga/) based on the hazard deaggregation . A further limitation of an amplitude scale factor in the range, $SF = 0.6$-1.6, was used to help ensure that ground motions with the correct frequency content (i.e. spectral shape) were selected.

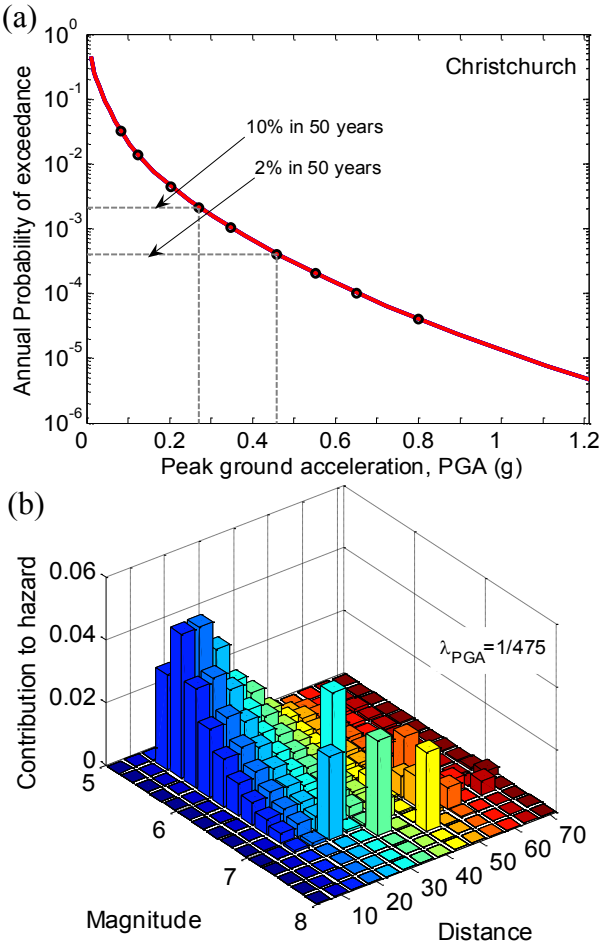

Figure 3: Details of the PGA seismic hazard for class C soil in Christchurch: (a) Seismic hazard curve; (b) Deaggregation of the hazard curve for an annual probability of exceedance of λ_{PGA}=1/475.

5 DETERMINISTIC PERFORMANCE ASSESSMENT

Before conducting the probabilistic seismic response analyses with multiple ground motions and at multiple intensity levels, it is necessary to first rigorously examine the computational model and its response to various levels of ground motion excitation. This is important for: (i) verification of the analysis algorithms, (ii) validation of the computational model with engineering judgment and observations, and (iii) to understand the predominant deformation mechanisms which control the response. The latter point, in particular, is necessary before conducting probabilistic effective stress analyses since the number of analyses means it is not feasible to examine each analysis in detail, with various engineering demand parameter (EDP's) simply used to indicate the

seismic response. Thus an understanding of the deformational mechanism is critical in the selection of appropriate EDP's, and below the seismic response of the computational model is illustrated for a single ground motion scaled to an intensity level with a 2% probability of exceedance in 50 years (i.e. 0.463g *PGA* from Figure 3a).

5.1 *Foundation soil response*

Figure 4 illustrates the development of excess pore pressures and eventual liquefaction in the soil surrounding the bridge. It can be seen that pore pressure ratios in the range $EPWPR = 0.2\text{-}0.5$ first develop in the bottom $N_1 = 10$ layer on the left hand side of the model, and at the base of the $N_1 = 15$ layer on the right hand side of the model. The bottom $N_1 = 10$ layer has almost entirely liquefied by 6.0 seconds. As time progresses, pore water pressures continue to increase in the $N_1 = 15$ layer on the right hand side of the model, and the re-distribution of excess pore pressures causes liquefaction to spread to shallower depths (predominantly on the left hand side of the model).

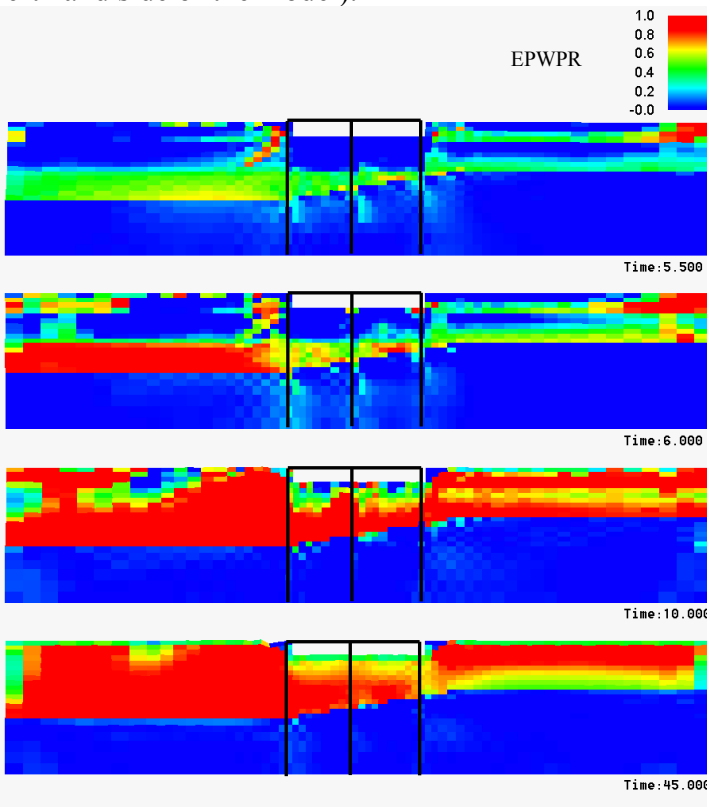

Figure 4: Development of excess pore water pressures and eventual liquefaction in the model during the deterministic analysis.

Figure 5a illustrates excess pore water pressure ratios 45 m to the left of the bridge. The three depths of $z = 6.15$, 14.75, and 19.75 m are located in the $N_1 = 15$, 10, and 30 layers, respectively. It can be seen that complete liquefaction of the $N_1 = 10$ (i.e. $z = -14.75$m) layer by 7.0 s causes the removal of high frequency waves in the upper 10 m of the model. The liquefaction of the bottom $N_1 = 10$ layer also reduces the ground motion intensity in the above soil layers, which prevents full liquefaction from eventuating at z = -6.15m. Figure 5b illustrates the shear stress-strain response of the soil at $z = -14.75$m. It can be seen that following dilation to a shear stress of ~63 kPa, the soil liquefies and the response is characterised by very low shear stiffness and shear strains up to 2.5%.

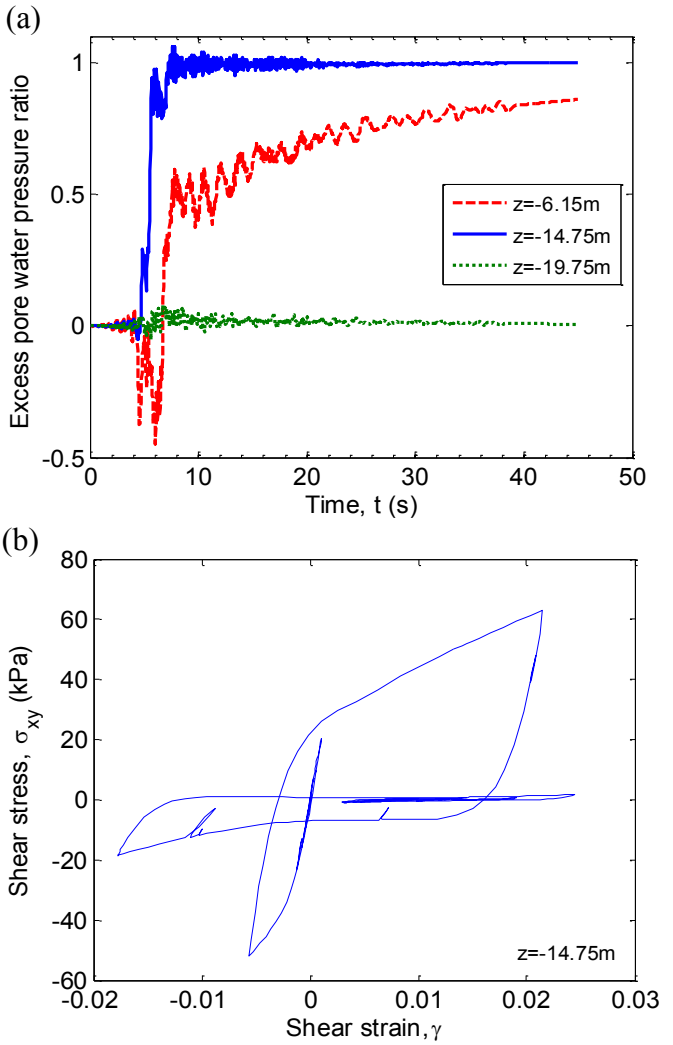

Figure 5: (a) Typical excess pore water pressure ratio development in the north free field (x=20 m in Figure 2); and (b) shear stress-strain response.

5.2 *Bridge and pile response*

Figure 6a illustrates the displacement time histories at the three footings of the bridge, and the north and south free-field response (all at a depth of $z = -3.2$ m). In the first 7.0 s, it is apparent that the displacement in the north free-field is larger than the south free-field and footing displacements, which are essentially identical. After 7.0 s relative displacements between the three footings becomes apparent due to significant liquefaction occurring in the surrounding soils. It is also apparent in Figure 6a that the displacement histories of the footings appear to be not completely in-phase with the free-field responses (both north and south). Figure 6b provides a comparison of the acceleration histories at the north free-field ($z = 0$ m), central pile cap, and

at 27.5 m depth, near the base of the model. It can be seen that the stiffening effect of the pile foundations allows waves of significantly higher amplitude and frequency to propagate to the central pier cap than to the free-field surface, thus the reason for the aforementioned out-of-phasing and smaller amplitude of the footing displacements in Figure 6a compared to that in the free-field.

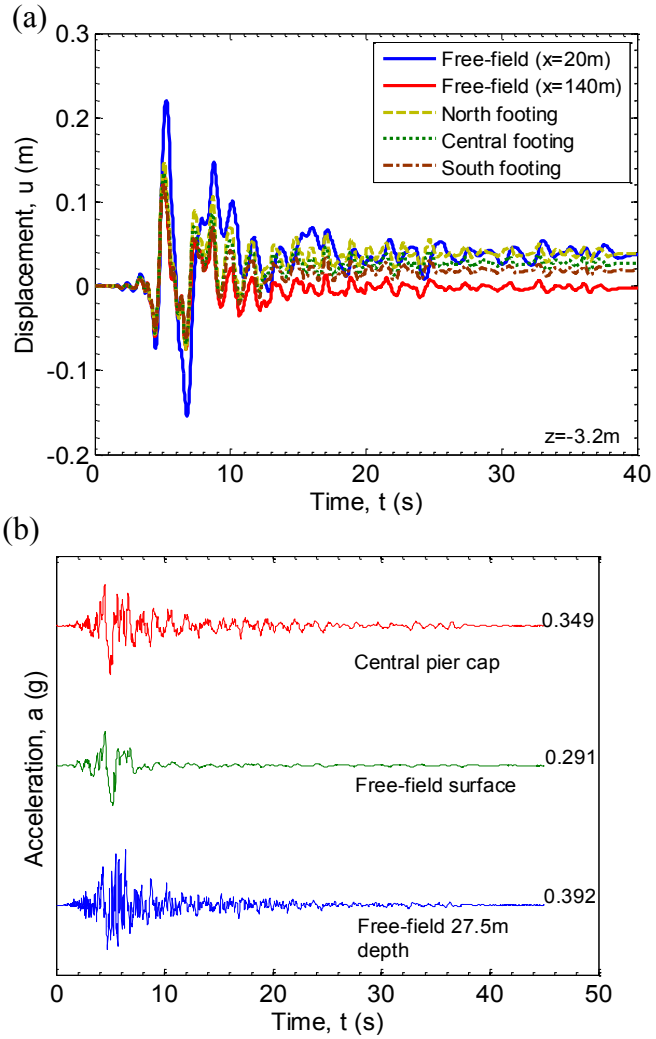

Figure 6: (a) displacement response history of the free field and at the pile footings; and (b) comparison of input, free-field, and pier cap acceleration histories (peak values given on the right hand side).

Figure 7a illustrates the bending moment profiles in piles and abutments/pier at $t = 5.15$ s which corresponds to the peak footing displacements in Figure 6a. It can be seen that the seismic demand on the pile foundations is significant with both north and central piles exceeding their respective yield moments, and the south pile exceeding the cracking moment. The variation in the $N_1 = 10$ - $N_1 = 30$ boundary depth (e.g. Figure 2) is also observed to have a pronounced effect on the depth at which the peak negative bending moment is developed in the piles. The effect of this depth variation also causes larger soil displacements on the north side of the model relative to the south. As the large axial stiffness of the bridge superstructure effectively enforces equal displacements of the top of the abutments (with the exception of seating displacement discussed in the next paragraph), this variation in soil displacements in the horizontal direction also causes significantly different moments in the upper half of the piles and the abutments/pier. Figure 7b illustrates the shear force histories for the two abutments and central pier. It is immediately evident that forces in the north and south abutments are of opposite sign indicating that the bridge superstructure is predominately restraining the displacements of the north abutment/pile (where soil displacements are relatively large), and increasing the displacement of the south abutment/pile (where soil displacements are relatively smaller).

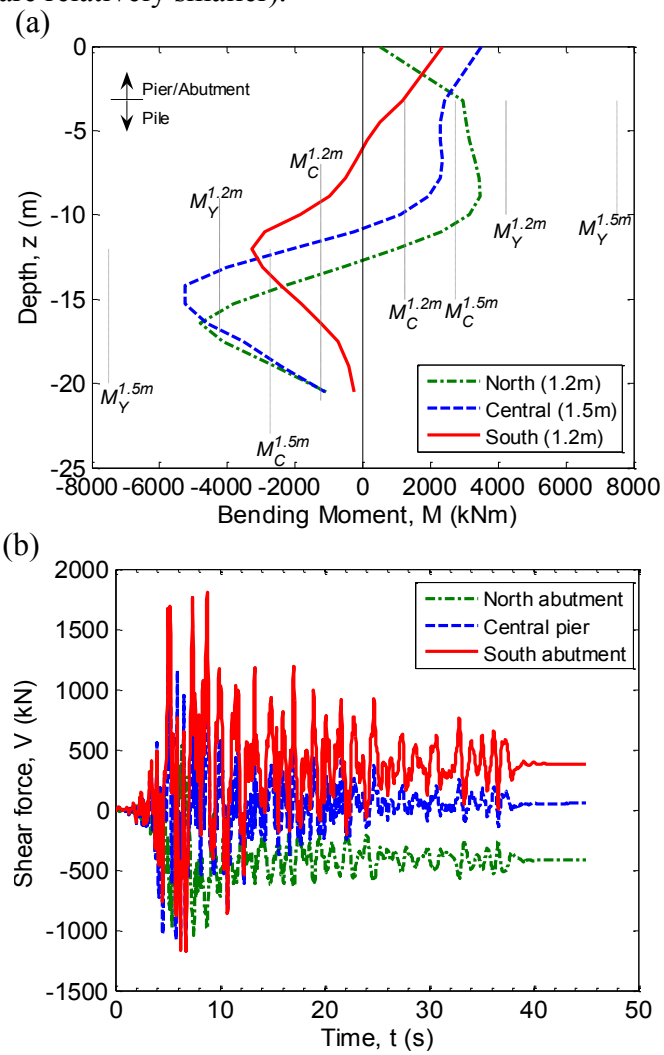

Figure 7: (a) bending moment profiles of the pile foundations at t=5.15s (M_C, M_Y are the cracking and yielding moments, respectively); and (b) shear force time histories in the abutments/pier.

Figure 8 illustrates the relative displacement between the bridge superstructure and abutment (herein referred to as seating displacement) at the north and south abutments (the superstructure is fixed to the central pier). While for this particular ground motion the absolute value of the seating displacements are small (~1cm) compared with those necessary to cause unseating failure, this effect may be more important for higher levels of ground motion. In addition, correctly modelling the seating dis-

placement also restricts the maximum shear force which can be transmitted between the bridge superstructure and abutments, which was observed to reduce the bending moments in the north and south abutments relative to those in the central pier.

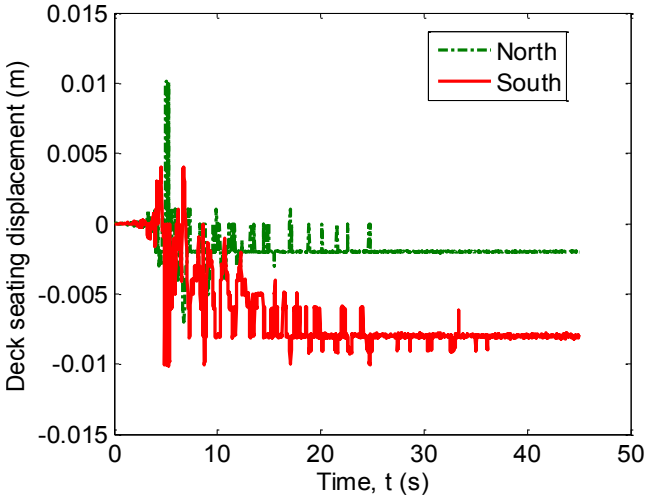

Figure 8: Deck seating displacement at the north and south abutments.

6 PROBABILISTIC SEISMIC RESPONSE AND SEISMIC DEMAND HAZARD

6.1 *Probabilistic seismic response analyses*

Clearly a vast amount of information and insight into the seismic response of the entire bridge-pile-soil foundation is possible by rigorously examining such seismic effective stress analyses discussed in the previous section. Based on the observations of various deterministic analyses, a total of nine different engineering demand parameters (EDP's) were monitored in each of the probabilistic seismic response analyses discussed in this section. These EDP's were: the peak curvature throughout the length of each of the three piles; the peak curvature in the abutments and central pier; the maximum seating displacement at the two abutments; and the maximum value of the settlement of the gravel approaches to the bridge superstructure. Due to space limitations only the EDP|IM plot for a single EDP is discussed below.

Figure 9 illustrates the results of the seismic response analyses for twenty ground motions at nine intensity levels for peak curvature in the north pile. Several points are worthy of note in Figure 9. Firstly, as expected the demand increases with an increase in the input ground motion intensity. Secondly, there is a large amount of dispersion in the results (e.g. for $PGA = 0.46$ g the peak curvature in the north pile ranges from 0.0004-0.005). This large dispersion occurs because of the acknowledged inefficiency of *PGA* as a ground motion intensity measure for the seismic response of soft soil deposits.

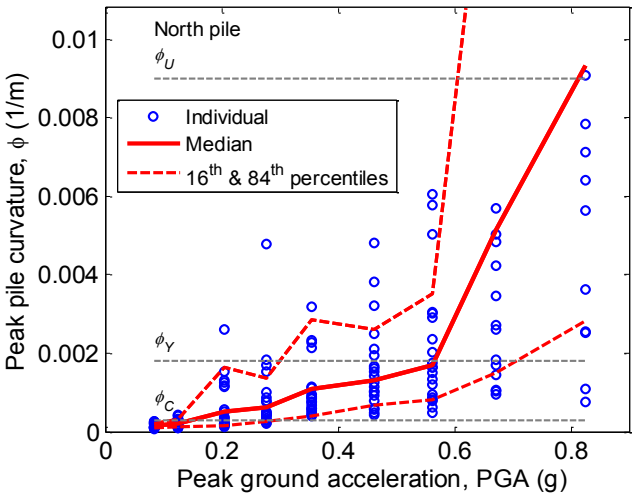

Figure 9: Example probabilistic seismic response analysis results for the north pile foundation.

6.2 *Seismic demand hazard*

By combining the seismic response analyses obtained in the previous section, which account for the variability in response due to the complexity of the ground motion excitation, with the seismic hazard curve in Figure 3a it is possible to compute the demand hazard curve for each of the different EDP's monitored. The demand hazard curve gives the annual frequency of exceeding a specified level of demand. Mathematical details can be found in Bradley et al. (2009b).

Figure 10a illustrates the demand hazard curves for peak pile curvature for each of the three piles in the computational model. The effect of the variation in demand for the piles observed in Figure 9 is also apparent in the demand hazard curves. Based on the monotonic moment-curvature relationship of the piles, cracking, yielding, and ultimate damage states are also given in Figure 10a. It can be seen that the north and south piles are more vulnerable (i.e. have higher damage state exceedance frequencies) than the larger central pile, with the north pile significantly more vulnerable than the south pile, for higher levels of curvature. Figure 10b illustrates the demand hazard curves for the peak curvature of the abutments and central pier. It can be seen that the demand on the central pier is significantly greater than the north and south abutments, with the central pier having annual damage state exceedance frequencies typically an order of magnitude larger than the abutments.

Using relationships between demand, damage and loss for the nine demand measures used here it is possible to create loss hazard curves (loss vs. annual frequency of exceedance). Such loss hazard curves allow coupling of the likelihood of demand occurrence with the consequences of its occurrence, and are useful in communicating seismic risk to non-engineering stakeholders (Bradley et al. 2009b).

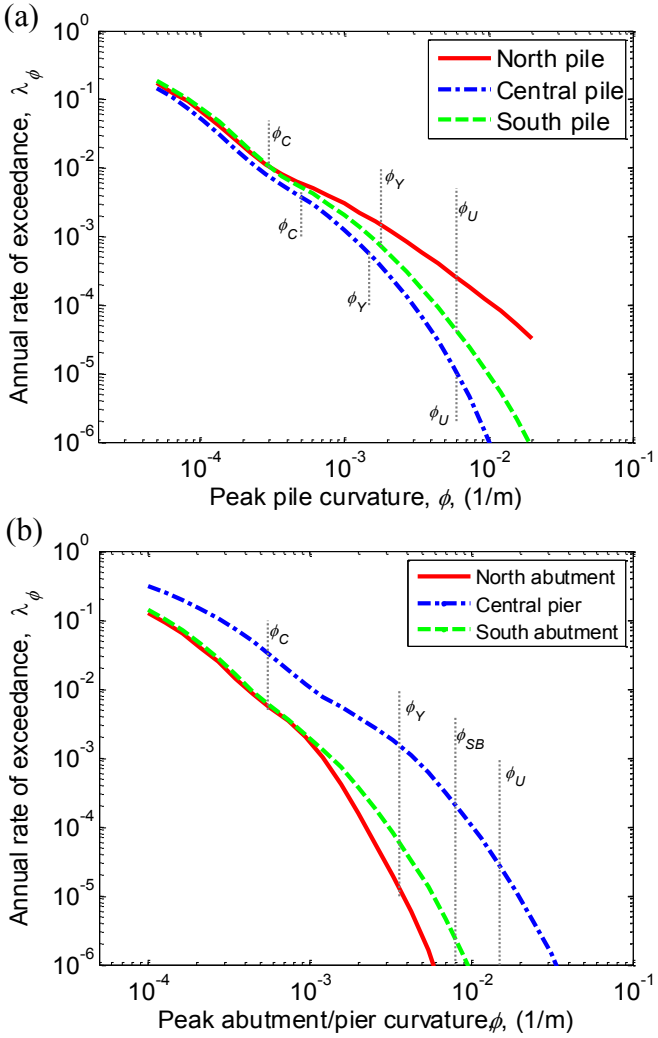

Figure 10: demand hazard curves for: (a) peak pile curvature; and (b) peak abutment/pier curvature.

7 PROBABILISTIC SEISMIC LOSS ASSESSMENT

The seismic risk of the bridge-foundation-soil system in terms of the explicit loss consequences due to structural response may be viewed as ultimate measures of seismic performance for decision making. In order to conduct such a seismic loss assessment, the consequences, in the form of direct repair cost and repair duration, due to various states of damage for each of the components of the system are required. To this end, a professional cost estimator was engaged to develop cost estimates and repair durations due to various levels of damage in each of the components of the Fitzgerald bridge (Hopkins 2009). For brevity only a brief summary of the loss assessment results are given below, and further details can be found in Bradley et al. (2010).

Figure 11 illustrates the deaggregations of the expected direct loss and downtime for the 2% in 50 year exceedance probability. It can be seen that the direct repair loss is primarily attributed to damage to the north piles, central pier and liquefaction of the approach embankments. Conversely, the cost to repair damage to the north and south abutments comprise a significantly smaller proportion of the total repair costs. Similar trends are also observed regarding the downtime deaggregation, except it is worthy of note that the total repair time for repair group 2, RG_2 (in particular, the central pier), is small considering the significance of the central pier in the deaggregation of the direct repair costs. This is because the duration required to repair cracking (using epoxy injection) in the central pier does not require excavation of the gravel backfills as in the case of repairing cracking in the bridge abutments. As for the direct repair cost, the downtime to repair damage in the north piles is larger than that for the central and south piles. The time to re-establish adequate seating length of the bridge deck at both the north and south abutments is also an important contributor to the total expected downtime of the bridge-foundation-soil system.

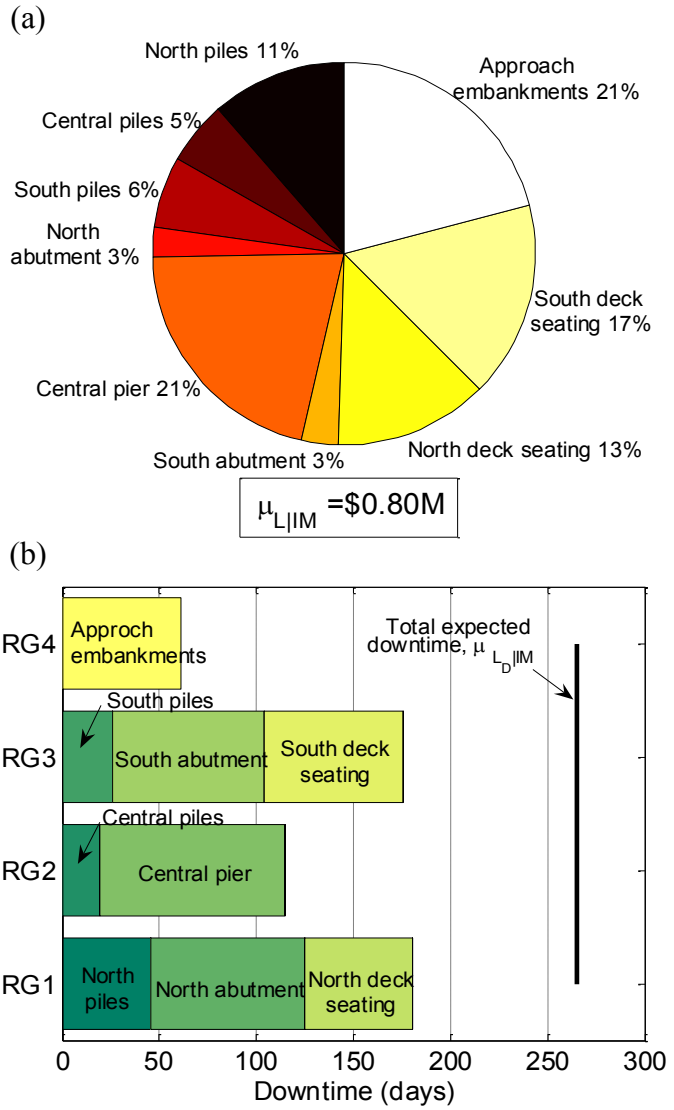

Figure 11: Deaggregation of the different components of the bridge-foundation-soil system for PGA = 0.46g (2% in 50 years) (a) the expected direct repair cost; and (b) expected downtime.

Knowing that travel delay and vehicle running costs due to inoperability of the bridge structure amount to $10,720/day (MWH 2008), the annual rate of exceeding a specified level of downtime (in

days) can be converted to the annual rate of exceeding a specified level of economic loss. Figure 12 illustrates the annual rate of exceeding some level of economic loss due to inoperability of the bridge, as well as the annual rate of exceeding some level of direct repair cost of the system. It can be seen that over the full range of economic losses, the economic implications due to loss of functionality is significantly larger than that due to direct repair of damage. In particular, the 2% in 50 year exceedance probability ($\lambda_L = 4.0\text{x}10^{-4}$) losses are \$1.20M and \$3.95M respectively. For comparative purposes it is again noted that the book-value of the Fitzgerald Avenue twin bridges is only \$2.4M. Thus, there is a 2% in 50 year probability that the total loss will exceed almost \$5.2M, over two-times the book-value of the infrastructure itself.

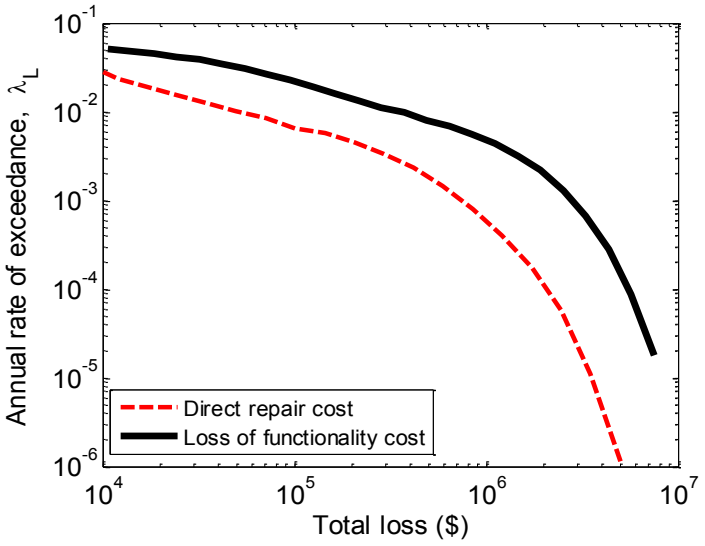

Figure 12: Comparison of the annual rate of exceedance of losses due to direct repair cost and loss of functionality.

8 CONCLUSIONS

This paper has presented the probabilistic seismic performance assessment of an actual bridge-foundation-soil system, the Fitzgerald Avenue twin bridges. The significant insight which can be gained regarding bridge-foundation-soil interaction and associated non-linearities using effective stress analysis was illustrated for a particular ground motion. The significant uncertainty regarding the input ground motion was addressed by subjecting the model to twenty different ground motions at nine different intensity levels. By combining the probabilistic EDP|IM relationships with the ground motion hazard curve, it is possible to compute the demand hazard for the various EDP's and compare them to various damage states for each of the components.

It was observed that the non-horizontal soil profile layering and soil liquefaction were key factors in the response of the bridge-foundation-soil system. The critical components governing the seismic performance of the system were the north abutment piles and the central pier, which had the highest annual frequencies of exceeding various damage states.

Loss analysis was used to provide further insight into the key components affecting the direct repair cost and downtime.

9 ACKNOWLEDGEMENTS

Financial support from the New Zealand Tertiary Education Commission and the New Zealand Earthquake Commission is greatly appreciated.

REFERENCES

Bowen, H. & Cubrinovski, M. (2008). Effective stress analysis of piles in liquefiable soil: A case study of a bridge foundation. *Bulletin of the New Zealand Society for Earthquake Engineering* 41(4): 247-262.

Bradley, B. A., Cubrinovski, M., Dhakal, R. P. & MacRae, G. A. (2009a). Intensity measures for the seismic response of pile foundations. *Soil Dynamics and Earthquake Engineering* 29(6): 1046-1058.

Bradley, B. A., Dhakal, R. P., Cubrinovski, M., MacRae, G. A. & Lee, D. S. (2009b). Seismic loss estimation for efficient decision making. *Bulletin of the New Zealand Society for Earthquake Engineering* 42(2): 96-110.

Bradley, B. A., Cubrinovski, M., Dhakal, R. P. & MacRae, G. A. (2010). Probabilistic seismic performance and loss assessment of a bridge-foundation-soil system. *Soil Dynamics and Earthquake Engineering*: DOI: 10.1016/j.soildyn.2009.12.012.

Cubrinovski, M. & Ishihara, K. (1998). Modelling of sand behaviour based on state concept. *Soils and foundations* 28(3): 115-127.

Cubrinovski, M. & Bradley, B. A. (2009). Evaluation of seismic performance of geotechnical structures. *International Conference on Performance-Based Design in Earthquake Geotechnical Engineering — from case history to practice*, Tokyo, Japan, 16.

Diana-J3. (1987). Finite-element program for effective stress analysis of two-phase soil medium. Software science.

Hopkins, W. (2009). Cost estimates for seismic damage to the Fitzgerald Avenue twin bridges. (personal communication).

MWH. (2008). Avonside/Fitzgerald/Kilmore Intersection: Economic Evaluation. Prepared for: Christchurch City Council, 42pp.

Shome, N. & Cornell, C. A. (1999). Probabilistic seismic demand analysis of nonlinear structures. *Report No. RMS-35, RMS Program*, Stanford University, Stanford, CA, 357pp.

Stirling, M. W., Gerstenberger, M., Litchfield, N., McVerry, G. H., Smith, W. D., Pettinga, J. R. & Barnes, P. (2007). Updated probabilistic seismic hazard assessment for the Canterbury region. *GNS Science Consultancy Report 2007/232, ECan Report Number U06/6*, 58pp.